

# Spatial and seasonal patterns of water isotopes in northeastern German lakes

Bernhard Aichner<sup>1</sup>, David Dubbert<sup>2</sup>, Christine Kiel<sup>3</sup>, Katrin Kohnert<sup>3</sup>, Igor Ogashawara<sup>3</sup>, Andreas Jechow<sup>2,3</sup>, Sarah-Faye Harpenslager<sup>1</sup>, Franz Hölker<sup>2</sup>, Jens Christian Nejtgaard<sup>3</sup>, Hans-Peter Grossart<sup>3,4</sup>, Gabriel Singer<sup>2,5</sup>, Sabine Wollrab<sup>3</sup>, Stella A. Berger<sup>3</sup>

<sup>1</sup> Leibniz Institute of Freshwater Ecology and Inland Fisheries, Dep. 2 Ecosystem Research, Müggelseedamm 301, Berlin, Germany

<sup>2</sup> Leibniz Institute of Freshwater Ecology and Inland Fisheries, Dep. 1 Ecohydrology, Müggelseedamm 310, Berlin, Germany

<sup>3</sup> Leibniz Institute of Freshwater Ecology and Inland Fisheries, Dep. 3 Experimental Limnology, Zur alten Fischerhütte 2, D-16775 Stechlin

<sup>4</sup> Potsdam University, Institute for Biochemistry and Biology, Maulbeerallee, D-14469 Potsdam, Germany

<sup>5</sup> Department of Ecology, Innsbruck University, Technikerstrasse 25, A-6020 Innsbruck, Austria

*Correspondence to:* Bernhard Aichner (bernhard.aichner@gmx.de)

**Abstract.** Water isotopes ( $\delta^{18}\text{O}$  and  $\delta^2\text{H}$  and  $\delta^{18}\text{O}$ ) were analyzed in samples collected in lakes associated to riverine systems in northeastern Germany throughout 2020. The dataset (Aichner et al., 2021) is derived from water samples collected at a) lake shores (sampled in March and July 2020); b) buoys which were temporarily installed in deep parts of the lake (sampled monthly from March to October 2020); c) multiple spatially distributed spots in four selected lakes (in September 2020); d) the outflow of Müggelsee (sampled biweekly from March 2020 to January 2021). At shores, water was sampled with pipette from 40-60 cm below water surface and directly transferred into a measurement vial, while at buoys a Limnos water sampler was used to obtain samples from 1 m below surface. Isotope analysis was conducted at IGB Berlin, using a Picarro L2130-i cavity ring-down spectrometer, with a measurement uncertainty of <0.04‰ ( $\delta^{18}\text{O}$ ) and <0.39‰ ( $\delta^2\text{H}$ ). The data give information about the full seasonal and vegetation period isotope amplitude in the sampled lakes and about spatial isotope variability in different branches of the associated riverine systems.

## 30 **1 Introduction**

The varying physical properties of stable oxygen and hydrogen isotopes of the water molecule ( $^{16}\text{O}$ ,  $^{17}\text{O}$ ,  $^{18}\text{O}$ ,  $^1\text{H}$ ,  $^2\text{H}$ ) result in isotope fractionation during evaporation and condensation processes. This causes spatial and temporal variability of the isotopic signature of water in both the liquid and the vapor phase (Craig, 1961; Dansgaard, 1964; Gat and Gonfiantini, 1981). Water stable isotopes are therefore ideal tracers of hydrological processes, for example in lacustrine and riverine systems. Specifically in lakes, their general morphology (water volume, lake area, depth and shape), the mean residence time of the water, the balance between in- and outflows of multiple types (surface water, groundwater, precipitation), and their connectivity to other water bodies, are important parameters controlling isotope ratios (Herzceg et al., 2003; Bocanegra et al., 2013; Wu et al., 2015; Kang et al., 2017, Mass-Dufresne et al., 2021).

40 The northeastern part of Germany is characterized by a complex system of rivers and lakes. The connectivity of those lakes is an important influence on how ecological and chemical water properties are propagated along the river-lake network. Water isotopes are ideal proxies to identify spatial patterns within these coupled riverine and lacustrine systems and therefore a potential tool to assess lake-to-lake connectivity. So far, available isotope data from this region are limited to large rivers (Reckert et al., 45 2017), punctual snapshot data (Richter and Kowski, 1990), or small-scale patterns in local settings (Kuhlemann et al., 2020; Vyse et al., 2020; Kleine et al., 2021).

Here, we provide a comprehensive dataset of water isotopes in lakes along the river-lake system of the northeastern German lowland area (Aichner et al., 2021), which covers the major riverine systems and evaluates the seasonal variability on selected spots, i.e. in lakes which are part of different riverine 50 branches of the investigated river systems. The two major questions are: a) What is the seasonal variability of water isotope values across the northeastern German lacustrine systems? b) Are there spatial trends that can be ~~unraveled~~unravelling by water isotope data?

For future regional studies, answers to these questions and the assessment if water stable isotopes can be used as accurate proxy for lake-to-lake connectivity, will be valuable in context of the potential 55 relationship between hydrological, chemical, and biological properties of the studied systems.

## 2 Study site

Northeastern Germany, a section of the glacially formed North German Lowland, is characterized by a complex system of rivers and 1000+ lakes (Fig. 1) with highly variable limnological features such as size, depth, shape and biogeochemical properties (Ogashawara et al., 2020; 2021). Most of these inland waters are a part of the Elbe watershed, discharging into the North Sea, with the Spree-Dahme system and the Müritz-Havel system as major tributaries. Further to the northeast the Ucker system forms a major cluster of rivers discharging into the Baltic Sea. Smaller natural and artificial channels add to the complexity of this riverine and lacustrine network.

The study area is situated in the temperate climate zone with an annual precipitation and temperature of approx. 600 mm and 10 °C, respectively (Berlin; DWD, 2021). Isotope values of precipitation range from -84‰ (January) to -49‰ (July) for  $\delta^2\text{H}$  and from -11.6‰ to -6.9‰ for  $\delta^{18}\text{O}$  (OIPC, Online Isotopes in Precipitation Calculator; ~~Bowen, 2022 and Wilkinsson, 2002~~; ~~Bowen and Revenaugh, 2003 et al., 2005~~; ~~IAEA/WMO, 2015~~; Stumpp et al., 2014). Due to continental and altitude effects, i.e. isotopic depletion with progressive transport and rain-out of water vapor,  $\delta$ -values of precipitation isotopes decrease in the eastern part of Germany from the NW to the SE. This trend is mirrored in groundwater  $\delta^2\text{H}$  values, which decrease in the study area from -60‰ in Lake Müritz to -63‰ in Spree-Dahme rivers (Richter, 1978; Richter and Kowski; 1990).

Lakes sampled for this study are listed in Tables 1 and 2 and can be clustered into nine geographical groups: I) Lake Müritz and Kölpinsee (Fig 1), which are discharging via the Erpe towards the NW to the Elbe (Fig. 1). II) Deep Müritz-Havel lakes (Fig. 2a), which discharge towards the SE and E before the confluence with the Upper Havel river in Priebertsee: Schwarzer See, Zethner See, Vilzsee, Zotzensee, Labussee, Rätzsee, Canower See, Kleiner Pälitzsee, Großer Pälitzsee. III) The mostly shallow Upper Havel lakes (Fig. 2b), located north of the confluence with the Müritz-Havel water ways: Zierker See, Useriner See, Großer Labussee, Woblitzsee, Großer Priepertsee. IV) Havel Lakes (Fig. 2d), east of the confluence: Ellbogensee, Ziernsee, Röblinsee and Stolpsee. V) Großer Lychensee, which is connected via the river Woblitz with the Stolpsee. VI) Feldberg Lakes: Feldberger Haussee, Breiter Luzin and Schmalter Luzin.(Fig. 2c), which are connected with each other via surface flow, but only via groundwater flow with the lakes of group V. VII) Lakes connected to the Ucker system, mostly via smaller creeks and

85 artificial channels (Fig 1 and 2c): Krewitzsee, Mellensee, Wrechner See, Großer See, Große Lanke  
(southernmost sector of Oberucker See), and Suckower Haussee. VIII) The Spree-Dahme system  
southeast of Berlin (Fig. 3): Spree, Dämeritzsee, Große Krampe, Dahme, and Müggelsee. IX) Individual  
lakes Stechlin, and Peetschsee, which are not connected to a major river, but for which connectivity via  
groundwater flow and small artificial channels is partly still of relevance.

90 All of these sampled lakes show variable morphometric and ecological characteristics (Tables 1 and 2).  
The water depths range from 3 m (Zierker See) to 70 m (Lake Stechlin and the volumes from approx. 5.6  
million to 99.6 million m<sup>3</sup> (same lakes). By lake area, the investigated water bodies range from small  
ponds such as Peetschsee (19.1 ha) to the largest German lake, the Müritz (10910 ha). Most of the studied  
northeastern German lakes are mesotrophic or eutrophic according to the classification of LAWA  
95 (LAWA, 2014; Table 1 and 2). Oligotrophic conditions only occur in the Lake Schmäler Luzin. The water  
residence time (WRT) in these lakes, i.e. the mean time that water spends in a particular lake, has been  
estimated by means of dividing the lake volume by the flow in or out of the lake (Wetzel, 2001). It ranges  
from a few weeks to few months in most river-connected lakes, while the Feldberg lakes and Lake  
Stechlin have longer residence times of ca. 3 to 16 years and >60 years, respectively (Table 2).

## 100 **3 Methods**

### **3.1 Water sampling**

Water samples were taken at the shore of 31 lacustrine and riverine spots from 40–60 cm water depth  
between 8<sup>th</sup>-10<sup>th</sup> March 2020 and 13<sup>h</sup>–19<sup>th</sup> July 2020 (Figs. 1–3; Table 1). At Müggelsee, samples were  
taken from a boat pier before the outflow on the northwestern side of the lake, in 2-4 weekly intervals  
105 between March 2020 and January 2021. Additionally, more samples were taken at two sites further east  
on the northern shore of the lake (Fig. 3) on 19<sup>th</sup> June and 13<sup>th</sup> July 2020. Water samples were taken with  
a pipette and directly transferred in a gas chromatography (GC)-vial, which was closed instantly after  
sampling and stored cold (6°C) until further processing.

Between March and October 2020, water samples from a subset of 19 lakes (Table 2), were taken in 1-2  
110 months intervals from a boat close to buoys, which were temporarily deployed as part of the project

CONNECT at the deepest point of the lake, or (if a site coincided with a water way) near to the outflow of the lake (Ogashawara et al. 2020, 2021): March: 17<sup>th</sup>–19<sup>th</sup>. May: 25<sup>th</sup>–28<sup>th</sup>. June/July: 29<sup>th</sup>–2<sup>nd</sup>. August: 3<sup>rd</sup>–6<sup>th</sup>. September: 1<sup>st</sup>–3<sup>rd</sup>. October: 5<sup>th</sup>–8<sup>th</sup>. On 29<sup>th</sup> and 30<sup>th</sup> September, four lakes (Zierker See, Großer Priepertsee, Ellbogensee, Röblinsee) were sampled at a higher spatial resolution, by taking six or seven surface samples, distributed over the whole lake surface area by positions close to all shores, in addition to the sample at the deepest point and / or ~~center~~centre of the lakes (Fig. 2).

A Limnos water sampler (Limnos.pl, Komorów, Poland), capturing 2.5 L volume, was used to obtain water samples from 1 m depth. Samples were transferred into 10 L canisters, closed after sampling and immediately transported to the lab. Canisters were carefully turned over-top ten times to guarantee constant mixing of samples before samples were transferred into GC-vials with a pipette for isotope analysis. Vials were stored in a cold room (6°C) in the dark until isotope measurement.

### 3.2 Isotope analysis

Water samples were filtered with 0.2 µm cellulose acetate (Faust Lab Science GmbH, Fabrikstraße 17, 79771 Klettgau, Germany) prior to analysis of stable isotopes ( $\delta^{18}\text{O}$  and  $\delta^2\text{H}$  values) in the water isotope lab at IGB Berlin, using a L2130-i cavity ring-down spectrometer (Picarro, Santa Clara, CA, USA). ~~Measurements were routinely checked for organic contamination using the Picarro ChemCorrect software. All measurements were post processed with the Picarro ChemCorrect™ software, which compared the measured spectra of the lab standards with the spectra of the samples. If statistical differences (i.e. baseline offset, spectral interference of organic compounds) between the two were too~~ high, a warning flag was assigned and the sample was excluded.

Isotope values and standard deviations are based on three replicate measurements of each sample, with additional three discarded measurements prior to avoid memory effects. To improve precision, all injections with a water concentration below 17,000 ppm and above 23,000 ppm, and with a standard deviation higher than 400 ppm of the measured water concentration across an injection's averaging window, were excluded.

For instrument calibration 3 laboratory standards for each group of 24 samples were used: L ( $\delta^{18}\text{O}$  - 17.86‰ and  $\delta^2\text{H}$  -109.91‰), DEL ( $\delta^{18}\text{O}$  -10.03‰ and  $\delta^2\text{H}$  -72.81‰), H ( $\delta^{18}\text{O}$  2.95‰ and  $\delta^2\text{H}$  0.29‰).

A fourth lab standard, M ( $\delta^{18}\text{O}$  -7.68‰ and  $\delta^2\text{H}$  -56.70‰), was used as quality and drift control after every 6 samples i.e. serving as lab-internal control and not being used for calibration. Mean values calculated from all measured M lab standards were -7.68‰ for  $\delta^{18}\text{O}$  with a SD of 0.10‰ and -55.93‰ for  $\delta^2\text{H}$  with a SD of 0.31‰. All lab standards were referenced against primary measurement standards: VSMOW2 (Vienna Standard Mean Ocean Water 2), GRESP (Greenland Summit Precipitation, and SLAP2 (Standard Light Antarctic Precipitation 2) from the IAEA (International Atomic Energy Agency, Vienna International Centre, A-1400 Vienna, Austria).

Based on error propagation from a) the uncertainty of reference lab standards, b) root mean square error of the calibration, and c) standard deviation of replicate measurements of standards and samples, the overall measurement uncertainty of water isotope analysis was quantified to <0.04‰ ( $\delta^{18}\text{O}$ ) and <0.39‰ ( $\delta^2\text{H}$ ).

## 4 Results and discussion

### 4.1 Time series

Isotopes exhibit a clear seasonal trend in the investigated lakes (Figs. 4 and 5). Minimum  $\delta^2\text{H}$  and  $\delta^{18}\text{O}$  values occur at the end of March / early April, while maximum values were measured at the end of September / early October. This is 6-8 weeks after the minimum and maximum water temperatures are reached, and independent from the annual trends of water pH and  $\text{O}_2$  saturation (Fig. 4). In the bi-weekly sampled Müggelsee, the isotope values vary from -53 to -44 ‰ ( $\delta^2\text{H}$ ) and from -7.2 to -5.3 ‰ ( $\delta^{18}\text{O}$ ), equivalent to seasonal isotope amplitudes of ca 9 ‰ and 1.9 ‰, respectively. The monthly sampled lakes, showed variable seasonal amplitudes (i.e. offsets between October and March), ranging from  $\delta^2\text{H}$  2–13 ‰ (average: 4 ‰) and  $\delta^{18}\text{O}$  0.4– 2.6 (average 0.9 ‰).

A seasonal isotopic signal has been observed in many riverine and lacustrine systems (e.g. Dutton et al., 2005; Ogrinc et al., 2011; Halder et al., 2015; Reckerth et al., 2017). Usually, the lake and river isotopes reflect the annual isotope trend of precipitation, but often with significant attenuation of the signal and delay of 1-3 months (Rodgers et al., 2005; Jasechko et al., 2016; Reckerth et al., 2017, Bittar et al., 2017).

This is in agreement with data from our study area, where precipitation isotopes reach their minimum and maximum in Dec/Jan and Jul/Aug, respectively, and exhibit a seasonal variability of ca 35 ‰ ( $\delta^2\text{H}$ ) and 4.7 ‰ ( $\delta^{18}\text{O}$ ) (OIPC data for Berlin; [Bowen and Revenaugh, 2003](#); [Bowen et al., 2005](#); [IAEA/WMO, 2015](#); [Bowen, 2022](#)). The reasons for the time delay between precipitation and river/lake water isotopes, and the smaller seasonal amplitude of the latter, can be attributed to multiple catchment characteristics and processes. Crucial influencing factors on how fast a precipitation isotope signal is transferred into fluvial systems, are the discharge regime of rivers and the area and topography of their catchment (Sklash et al, 1976; Malozewski et al., 1992; McGuire et al., 2005; Rodgers et al., 2005).

In our study area, the lowest seasonal (Mar-Oct) isotope variability was observed in Lake Stechlin, followed by the Feldberg lakes (Fig. 5), most likely due to their high water residence time and lack of connection to rivers (Table 2). In contrast, the highest amplitude is found in the shallow Zierker See, which also has the lowest volume of all studied lakes. Therefore it is most susceptible to summer evaporation with related isotopic enrichment of the lake water, and also to inflow events, causing more negative values, such as visible in March (Fig. 5). Lake morphology can similarly explain the wide [isotope](#) amplitude of Müggelsee (Fig. 4), which is relatively large in area but also among the ~~most~~ shallow of the studied lakes. Data from most Havel lakes, exhibited average seasonal isotope amplitudes (Figs 5 and 7). The Spree-Dahme locations, Kölpinsee and Müritzt, and the small Peetschsee, showed relatively large deviations between March and July (Fig. 7). All those lakes are either very shallow or have at least a large area to depth ratio.

These results show that the seasonal isotope amplitude is influenced by multiple characteristics of the studied lakes. Aside morphological parameters ~~such as~~ (lake area, depth, and volume), hydrological features ~~such as~~ (e.g. water residence time) are of importance.

## 4.2 Spatial patterns

In the four lakes with increased spatial coverage from September samples, little intra-lake variability of isotope values (0.5–1 ‰ for  $\delta^2\text{H}$  and 0–0.2 ‰ for  $\delta^{18}\text{O}$ ) was observed (Fig. 6). In contrast, along the transects, the multiple lakes showed an isotope variability of ca. 25‰ ( $\delta^2\text{H}$ ) (Fig. 7).

190 In general, lakes showed isotopic depletion (values becoming more negative) from the north-west (Müritz) towards the south-east (Spree-Dahme). This follows the similar spatial trend of isotopes in precipitation and groundwater (Richter, 1987; Richter and Kowski, 1990).

In addition, the lakes from the different geographical clusters can be distinguished according to their water isotope signatures: (I) highest values were measured in the two lakes associated with the Müritz-Erpe system (I). The Upper Havel is characterized by lower isotope values than the Müritz-Havel (II and III).  
195 An exception are the two lakes Schwarzer See and Zethner See, which show more negative values than the other Müritz-Havel lakes (Fig. 7). Those form a chain of headwater lakes in the Müritz-Havel system, whose major inflow is north of Zotensee (Fig. 2a). Schwarzer See is characterized by a comparably large mean residence time of lake water (Table 2), and is probably under increased influence of isotopically  
200 depleted groundwater. The influence of the different isotopic signatures of the two Upper Havel branches is also visible at their confluence in Ellbogensee (Fig. 2a). Here, two samples ELL 2 and ELL 3 (white squares in Fig. 6) taken before the Upper Havel, show approx. 1 ‰  $^2\text{H}$  enrichment, compared to the samples taken after the confluence. In general, the Havel lakes after the confluence (IV) carry a mixed isotope signature of the Müritz-Havel and Upper Havel, with stronger influence of the first, depending on  
205 season (Fig. 5–7). Isotope depletion was observed towards the Stolpsee, probably due to the influence of the Lychen lakes (V), which discharge into the Upper Havel at Stolpsee via the Woblitz river and which showed the most negative values of all sampled lakes in the Upper Havel system (Figs. 5 and 7).

The Feldberg Lakes (VI) are a group of lakes located approx. 35 km north-east of the Upper Havel system and with insignificant surface connection to the adjacent lake systems. They are characterized by  
210 relatively high water residence time and slow surface flow from Feldberger Haussee, to Breiter Lüzin, to Schmaler Lüzin.  $\delta^2\text{H}$  and  $\delta^{18}\text{O}$  values are higher compared to the Upper Havel and the main branch of the Havel (i.e. after the confluence at Gr. Priepertsee and Ellbogensee), yet these are typical values to the Müritz-Havel. Among the three lakes, Feldberger Haussee shows highest isotopic values, probably due

to its lower water depth and volume (compared to Breiter and Schmalzer Luzin) and therefore increased  
215 susceptibility to evaporative isotope enrichment.

Variable isotope values are observable in the six sampled lakes associated with the Ucker lake-river  
system (VII). Complex subsurface and surface flow patterns, mostly via smaller creeks and channels,  
their wide geographical distribution and variability in morphometric properties, can explain the isotopic  
heterogeneity in those lakes. A geographic trend, i.e. lower  $\delta^2\text{H}$  and  $\delta^{18}\text{O}$  values in the Oberuckersee  
220 (Große Lanke), compared to the more northern lakes (e.g. Mellensee, Krewitzsee) can be inferred from  
the data. The most negative isotope values in the study area were measured in samples from the lakes and  
rivers of the Spree-Dahme system (VIII), located approximately 100 km south-east of the Müritz-Havel-  
Ucker systems.

The final group of lakes is characterized by low surface flow connectivity to riverine systems and other  
225 lakes (IX). Those lakes (Lake Stechlin and Peetschsee) show higher isotopic values than adjacent lakes  
and rivers which can be attributed to evaporation effects. Those in turn are more pronounced in the smaller  
water bodies, which is visible at the large seasonal isotope amplitude in Peetschsee, compared to small  
seasonal variability in the deep and large Lake Stechlin (Fig. 7).

## 5 Conclusions

230 Stable isotope  $\delta^2\text{H}$  and  $\delta^{18}\text{O}$  values of water samples collected in northeastern German lakes and rivers  
show clear spatial and seasonal trends. While isotope data exhibit a tendency from relatively high values  
in the north-west, towards lower values in the south-east, evaporation and groundwater inflow influence  
the isotope values on a local scale. In this context, morphometric parameters (water depth, area, volume,  
and overall shape) and related hydrological properties (water residence time, susceptibility to lake water  
235 evaporation and groundwater inflow) are crucial features, with effects on both absolute isotope values  
and their seasonal amplitude.

The comprehensive dataset of stable water isotopes and lake morphological characteristics described here  
can help to set biological and biogeochemical data in context to hydrological processes in the northeastern  
German riverine and lacustrine systems. The ecological and chemical characteristics of these lake-river

240 systems are driven by a) connectivity between the lakes associated to river systems, in addition to b) local  
influencing factors which in turn often depend on lake morphology. Water isotopes are able to reflect  
both those aspects as shown by the different isotope patterns in the different branches of the Müritz-  
Havel-Ucker-Spree-Dahme system.

## **Author contributions**

245 B.A. designed the isotope study and wrote the manuscript in close cooperation with the CONNECT  
Project, coordinated by S.A.B., S.W., and performed by C.K., A.J., K.K., I.O., J.C.N., H.-P.G., F.H., G.S.,  
S.W., and S.A.B.. D.D. analyzed water samples collected by B.A., S.-F.H., K.K., C.K., I.O., A.J., S.A.B.,  
S.W., J.C.N., H.-P.G. and F.H.. All co-authors contributed to data evaluation and interpretation, and  
editing of the manuscript.

250

## **Acknowledgements**

We thank Solvig Pinnow, Gregorio Lopez Mazacotte, Bianca Schmid-Paech, Fabian Göppel, Maren  
Lentz, Gary Gottschall for help with sampling and sample preparation for isotope analysis. Funding was  
provided by German Science Foundation (DFG) (project Ai 134/3-1). Part of this work was funded by  
255 the Leibniz Association within the Collaborative Excellence programme for the project CONNECT –  
Connectivity and synchronisation of lake ecosystems in space and time (K45/2017).

## **Competing interests**

The authors declare no competing interests.

## **Data availability**

260 All data in this manuscript are available at PANGAEA: <https://doi.org/10.1594/PANGAEA.935633>

(Aichner et al., 2021; accessible after acceptance of this manuscript). Temporarily, the dataset can be accessed under this barrier free link:

<https://www.pangaea.de/tok/1da04ef79674dd9169df42db2368107323ee4ef4>

## References

- 265 Aichner, B., Dubbert, D., Kiel, C., Kohnert, K., Ogashawara, I., Jechow, A., Harpenslager, S. F., Hölker, F., Singer, G., Grossart, H. P., Nejstgaard, J. C., Wollrab, S., Berger, S. A.: Water isotope values from northeastern German lake systems. PANGAEA, <https://doi.org/10.1594/PANGAEA.935633>, 2021
- Bittar, T. B., Berger, S. A., Birsa, L. M., Walters, T. L., Thompson, M. E., Spencer, R. G. M., Mann, E. L., Stubbins, Al, Frischer, M. E., and Brandes. J.A.: Seasonal dynamics of dissolved, particulate and microbial components of a tidal saltmarsh-dominated estuary under contrasting levels of freshwater discharge, *Estuarine Coastal Shelf Sci.*, 182, Part A, 72-85, <https://doi.org/10.1016/j.ecss.2016.08.046>, 2016.
- 270 Bocanegra, E., Quiroz Londoño, O. M., Martínez, D. E., and Ro-manelli, A.: Quantification of the water balance and hydro-geological processes of groundwater–lake interactions in thePampa Plain, Argentina, *Environ. Earth Sci.*, 68, 2347–2357,<https://doi.org/10.1007/s12665-012-1916-4>, 2013.
- 275 ~~Bowen, G. J. and Wilkinson B.: Spatial distribution of  $\delta^{18}\text{O}$  in meteoric precipitation, *Geology*, 30(4), 315–318, [https://doi.org/10.1130/0091-7613\(2002\)030<0315:SDOIM>2.0.CO;2](https://doi.org/10.1130/0091-7613(2002)030<0315:SDOIM>2.0.CO;2), 2002.~~
- ~~Bowen, G. J. The Online Isotopes in Precipitation Calculator, version 3.1. <http://www.waterisotopes.org>. 2022.~~
- ~~Bowen G. J. and Revenaugh J.: Interpolating the isotopic composition of modern meteoric precipitation, *Water Resour. Res.*, 39(10), 1299, <https://doi.org/10.1029/2003WR002086>, 2003.~~
- 280 ~~Bowen G. J., Wassenaar L. I. and Hobson K. A.: Global application of stable hydrogen and oxygen isotopes to wildlife forensics. *Oecologia* 143, 337-348, doi:10.1007/s00442-004-1813-y, 2005.~~
- Craig, H.: Isotopic variations in meteoric waters, *Science*, 133, 1702–1703, doi:10.1126/science.133.3465.1702, 1961.
- Dansgaard, W.:Stable Isotopes in precipitation, *Tellus*, 16,436–68, <https://doi.org/10.1111/j.2153-3490.1964.tb00181.x>, 1964.
- 285 Dutton, A., Wilkinson, B.H., Welker, J.M., Bowen, G.J., and Lohmann, K.C.: Spatial distribution and seasonal variation in  $18\text{O}/16\text{O}$  of modern precipitation and river water across the conterminous USA, *Hydrol. Process.*, 19, 4121–4146. <http://dx.doi.org/10.1002/hyp.5876>, 2005.

- DWD, <https://www.dwd.de/DE/leistungen/klimadatendeutschland/klimadatendeutschland.html> accessed 7th May 2021, 2021.
- Gat, J.R., and Gonfiantini, R. (eds.): *Stable Isotope Hydrology: Deuterium and Oxygen-18 in the Water Cycle*. IAEA Technical Report Series No. 210. IAEA: Vienna, 1981
- Halder, J., Terzer, S., Wassenaar, L.I., Araguás-Araguás, L.J., and Aggarwal, P.K.: The Global Network of Isotopes in Rivers (GNIR): integration of water isotopes in watershed observation and riverine research, *Hydrol. Earth Syst. Sci.*, 19, 3419–3431. <http://dx.doi.org/10.5194/hess-19-3419-2015>, 2015.
- Herczeg, A. L., Leaney, F. W., Dighton, J. C., Lamontagne, S., Schiff, S. L., Telfer, A. L., and English, M. C.: A modern isotoperecord of changes in water and carbon budgets in a groundwater-fed lake: Blue Lake, South Australia, *Limnol. Oceanogr.*, 48, 2093–2105, <https://doi.org/10.4319/lo.2003.48.6.2093>, 2003. Jasechko, S., Kirchner, J.W., Welker, J.M., and McDonnell, J.J.: Substantial proportion of global streamflow less than three months old, *Nat. Geosci.*, 9 (2), 126–129. <http://dx.doi.org/10.1038/ngeo2636>, 2016.
- [IAEA/WMO: Global Network of Isotopes in Precipitation. The GNIP Database. Accessible at: https://nucleus.iaea.org/wiser, 2015.](https://nucleus.iaea.org/wiser)
- [IGB: Müggelsee measuring station data. https://emon.igb-berlin.de/grosser\\_mueggelsee.html, 2022.](https://emon.igb-berlin.de/grosser_mueggelsee.html)
- Kang, S., Yi, Y., Xu, Y., Xu, B., Zhang, Y.: Water Isotope framework for lake water balance monitoring and modelling in the Nam Co Basin, Tibetan Plateau, *J. Hydrol. Reg. Studies*, 12, 289-302, <https://doi.org/10.1016/j.ejrh.2017.05.007>, 2017
- Kleine, L., Tetzlaff, D., Smith, A., Goldammer, T. and Soulsby, C.: Using isotopes to understand landscape-scale connectivity in a groundwater-dominated, lowland catchment under drought conditions, *Hydrol. Process.*, 35(5). e14197. <https://doi.org/10.1002/hyp.14197>, 2021.
- Kuhlemann, L-M, Tetzlaff, D, and Soulsby, C.: Urban water systems under climate stress: An isotopic perspective from Berlin, Germany. *Hydrol. Process.*, 34, 3758–3776. <https://doi.org/10.1002/hyp.13850>, 2020.
- LAWA. Trophieklassifikation von Seen. Richtlinie zur Ermittlung des Trophie-Index nach LAWA für natürliche Seen, Baggerseen, Talsperren und Speicherseen. Empfehlungen Oberirdische Gewässer, edited by: Riedmüller, U., Bund/Länder Arbeitsgemeinschaft Wasser, LAWA, Munich, Germany, 2014.
- Maloszewski, P., W. Rauert, P. Trimborn, A. Herrmann, and Rau, R.: Isotope hydrological study of mean transit times in an alpine basin (Wimbachtal, Germany), *J. Hydrol.*, 140, 343–360, [https://doi.org/10.1016/0022-1694\(92\)90247-S](https://doi.org/10.1016/0022-1694(92)90247-S), 1992

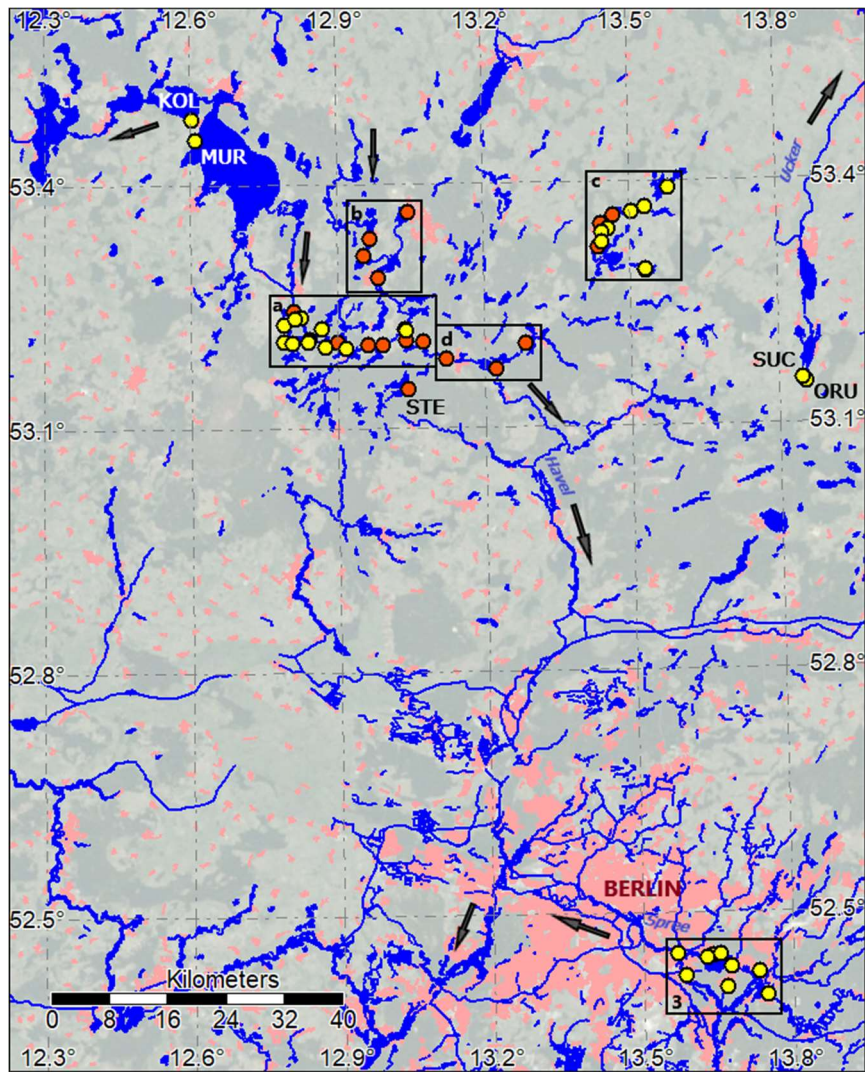
- Masse-Dufresne, J., Barbecot, F., Baudron, .P., and Gibson, J: Quantifying floodwater impacts on a lake water budget via volume-dependent transient stable isotope mass balance. *Hydrol. Earth Syst. Sci.* . 25, 3731-3757, 320 <https://doi.org/10.5194/hess-25-3731-2021>, 2021
- McGuire, K. J., McDonnell, J. J., Weiler, M., Kendall, C., McGlynn, B. L., Welker, J. M., and Seibert, J.: The role of topography on catchment-scale water residence time, *Water Resour. Res.*, 41, W05002, <https://doi.org/10.1029/2004WR003657>, 2005.
- Ogashawara, I., Jechow, A., Kiel, C., Kohnert, K., Berger, S.A., and Wollrab, S.: Performance of the Landsat 8 325 provisional aquatic reflectance product for inland waters, *Remote Sens.*, 12, 2410, <https://doi.org/10.3390/rs12152410>, 2020.
- Ogashawara, I., Kiel, C., Jechow, A., Kohnert, K., Ruutz, T., Grossart, H.-P., Hölker, F., Nejtgaard, J.C., Berger, S.A., and Wollrab, S.: The Use of Sentinel-2 for Chlorophyll-a Spatial Dynamics Assessment: A Comparative Study on Different Lakes in Northern Germany, *Remote Sens.*, 13, 1542. <https://doi.org/10.3390/rs13081542>, 2021.
- 330 Ogrinc, N., Kanduc, T., Miljevic, N., Golobocanin, D., and Vaupotic, J.: Isotope Tracing of Hydrological Processes in River Basins: The Rivers Danube and Sava. In: *Monitoring Isotopes in Rivers: Creation of the Global Network of Isotopes in Rivers (GNIR)*. edited by: International Atomic Energy Agency, Vienna, Austria, 187–196, 2012.
- Reckerth, A., Stichler, W., Schmidt, A., and Stumpp, C.: Long-term data set analysis of stable isotopic composition in German rivers, *J. Hydrol.*, 552, 718– 731. <https://doi.org/10.1016/j.jhydrol.2017.07.022>, 2017.
- 335 Richter, W.: Deuterium and Oxygen-18 in Central European Groundwaters, *Isotopes Environ. Health Stud.*, 23(11), 385-390, <https://doi.org/10.1080/10256018708623855>, 1987.
- Richter, W. and Kowski, P.: Deuterium and Oxygen-18 in Surface Waters of GDR draining to the Baltic Sea, *Isotopes Environ. Health Stud.*, 26(12), 569-573, <https://doi.org/10.1080/10256019008622436>, 1990.
- Rodgers, P., Soulsby, C., Waldron, S., and Tetzlaff, D.: Using stable isotope tracers to assess hydrological flow 340 paths, residence times and landscape influences in a nested mesoscale catchment, *Hydrol. Earth Syst. Sci.*, 9, 139–155, <https://doi.org/10.5194/hess-9-139-2005>, 2005.
- Sklash, M. G., Farvolden, R. N., and Fritz, P.: A conceptual model of watershed response to rainfall developed through the use of oxygen-18 as a natural tracer, *Canadian Journal of Earth Science*, 13, 271–283, <https://doi.org/10.1139/e76-029>, 1976.
- 345 Stumpp, C., Klaus, J., and Stichler, W.: Analysis of long-term stable isotopic composition in German precipitation. *J. Hydrol.*, 517, 351– 361, <https://doi.org/10.1016/j.jhydrol.2014.05.034>, 2014.

Vyse, S.A., Taie Semiromi, M., Lischeid, G., and Merz, C.: Characterizing hydrological processes within kettle holes using stable water isotopes in the Uckermark of northern Brandenburg, Germany, *Hydrol. Process.*, 34, 1868–1887, <https://doi.org/10.1002/hyp.13699>, 2020.

350 Wetzel, R. G, *Limnology, Lake and River Ecosystems*, 3rd Edition. New York: Academic Press, 2001.

Wu, H., Li, X., Li, J., Jiang, Z., Li, G., and Liu, L.: Evaporative enrichment of stable isotopes ( $\delta^{18}\text{O}$  and  $\delta\text{D}$ ) in lake water and the relation to lake-level change of Lake Qinghai, Northeast Tibetan Plateau of China. *J. Arid Land* 7, 623–635, <https://doi.org/10.1007/s40333-015-0048-6>, 2015

355



360 **Figure 1: Sampling locations in the lakes at the shores (yellow) and at the buoys (red). Arrows indicate major flow directions of rivers. Black boxes refer to detailed maps in Fig 2 and 3. Underlying map © Google Maps 2021.**

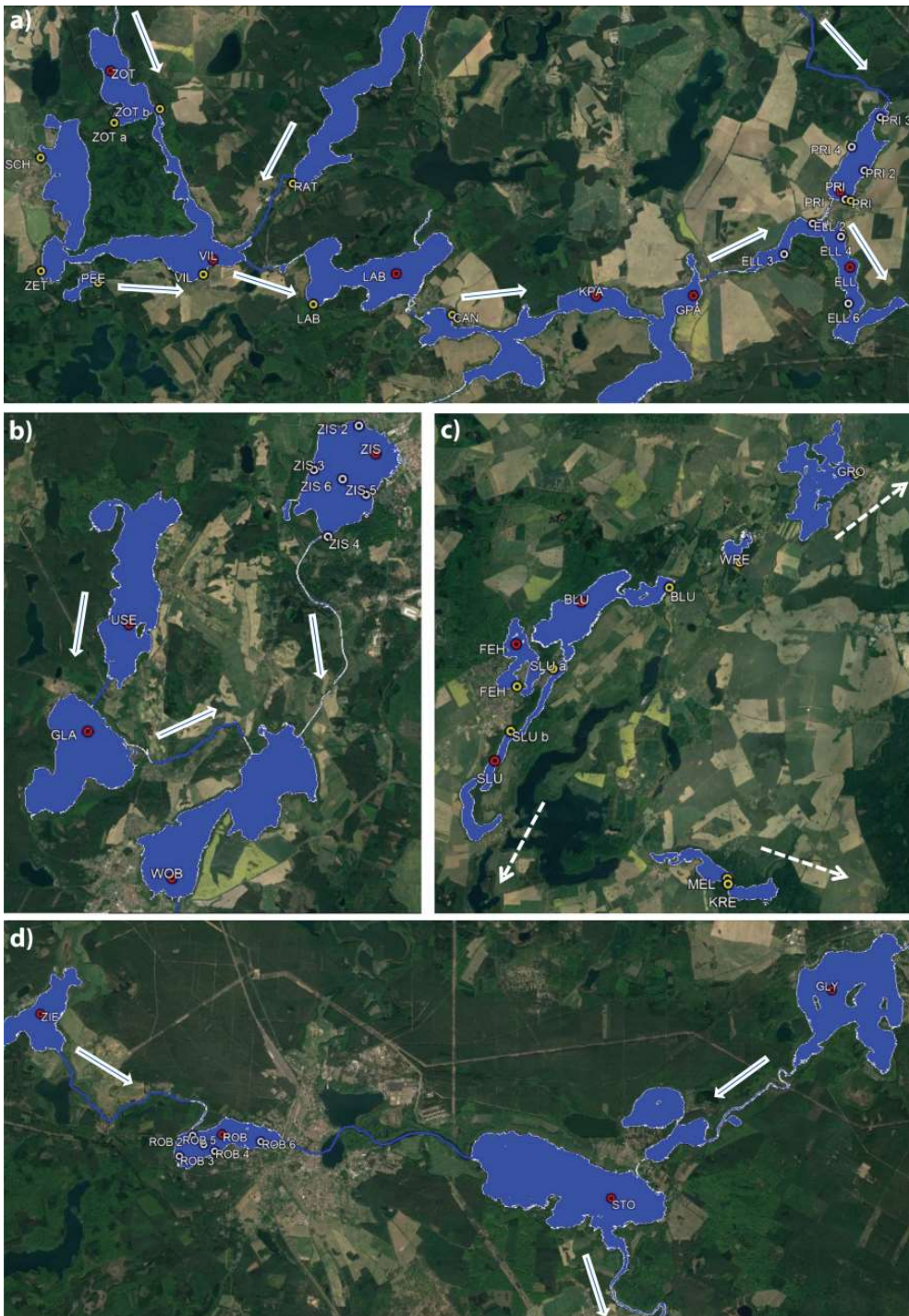
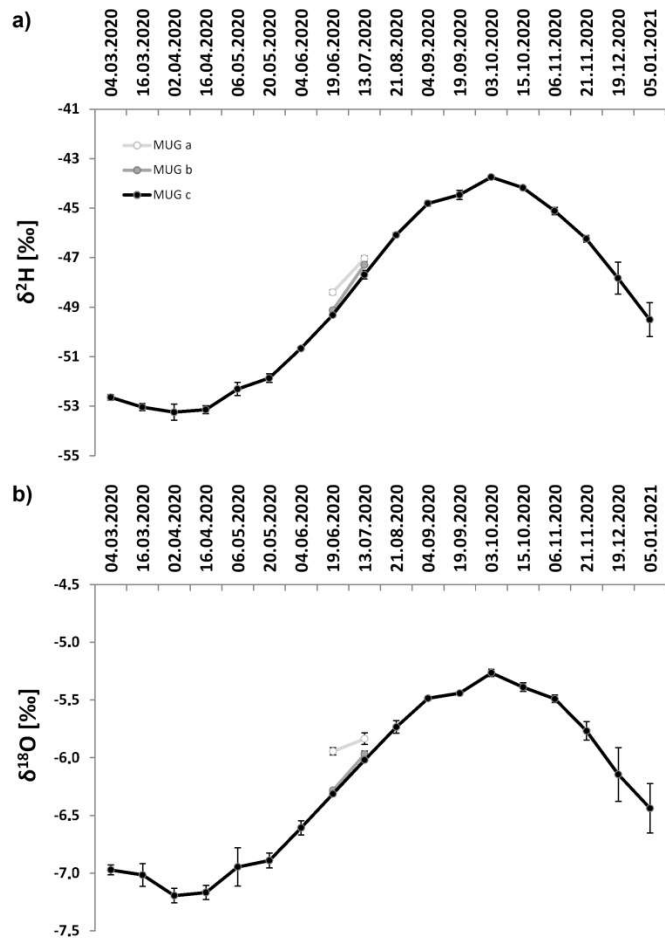
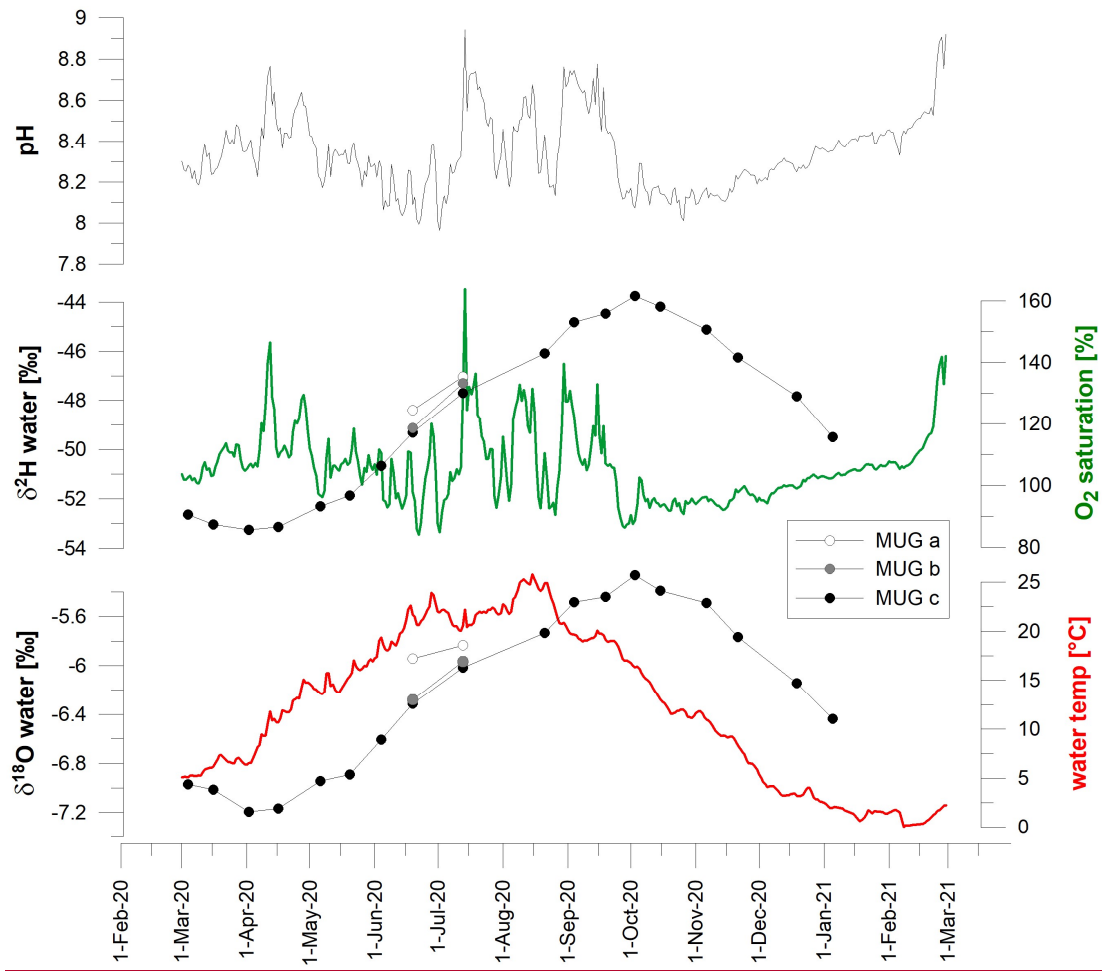


Figure 2: Sampling locations at (a) the Müritz-Havel, (b) the Upper Havel, (c) in Feldberg Lakes, (d) the Havel main branch. Shore samples taken in March and July 2020 marked yellow. Time series samples from buoys in red. Arrows indicate stream flow direction. Underlying map © Google Earth 2021.



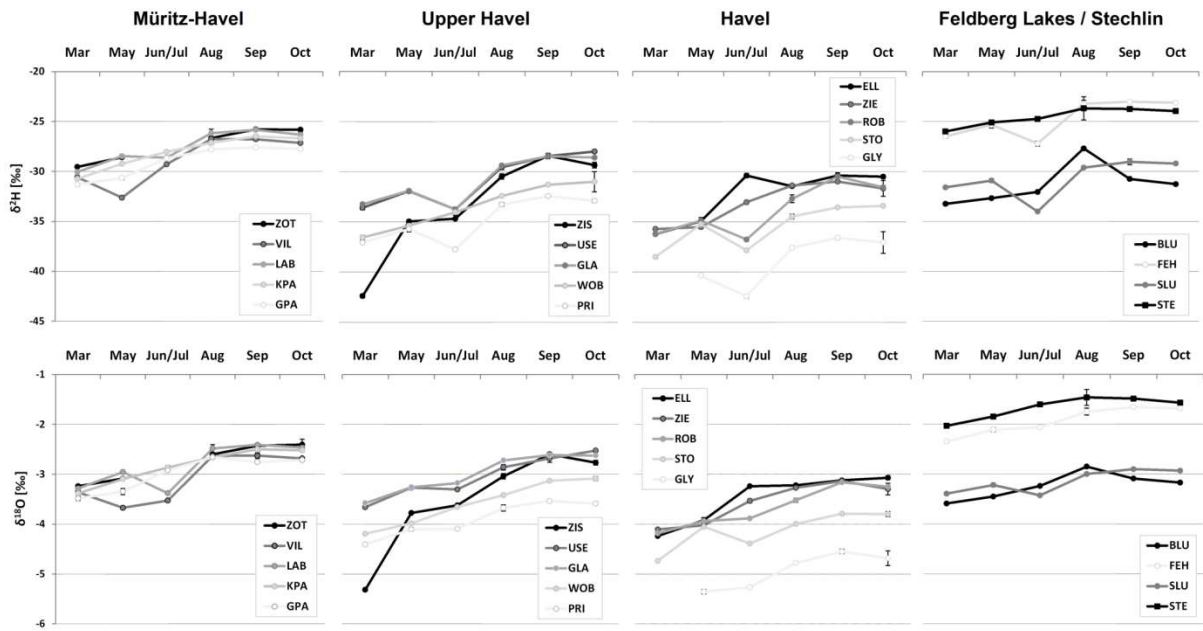
Figure 3: Sampling locations at the Spree-Dahme. Time series samples from the Müggelsee outflow in red. Arrows indicate stream direction. Underlying map © Google Earth 2021.





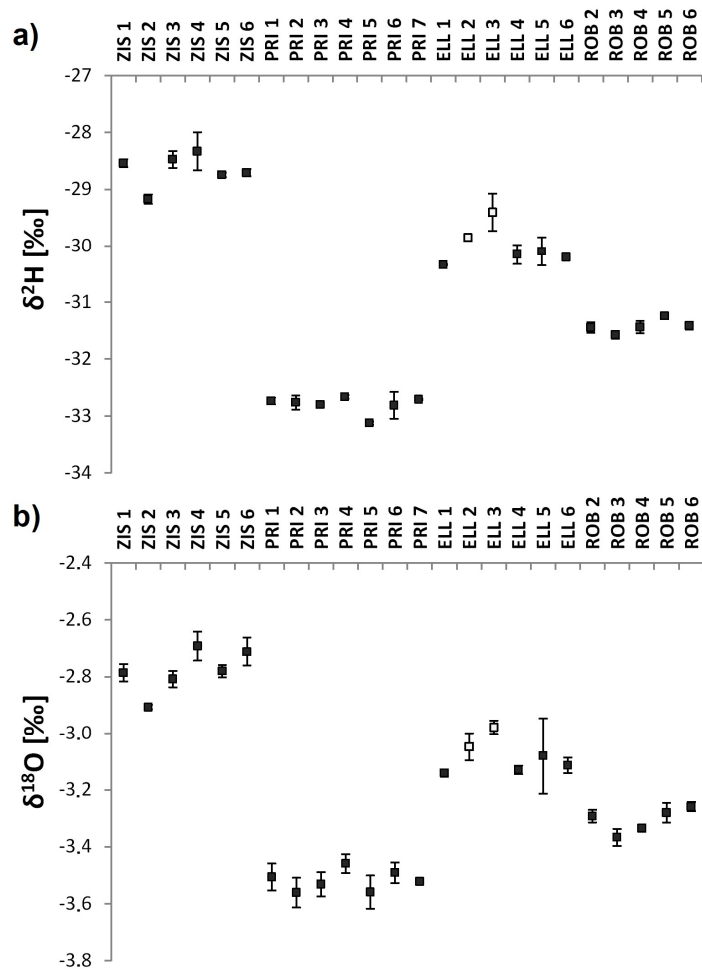
380

Figure 4: Timeseries of  $\delta^2\text{H}$  and  $\delta^{18}\text{O}$  values from the samples taken in 2-4 weekly intervals (March 2020 – January 2021) at the outflow of Müggelsee (MUG c: Friedrichshagen ~~harbor~~harbour) and from additional samples taken on the northern shore (MUG a and b) on 19<sup>th</sup> June and 13<sup>th</sup> July. [Water chemical data from the IGB measuring station \(IGB, 2022\).](#)

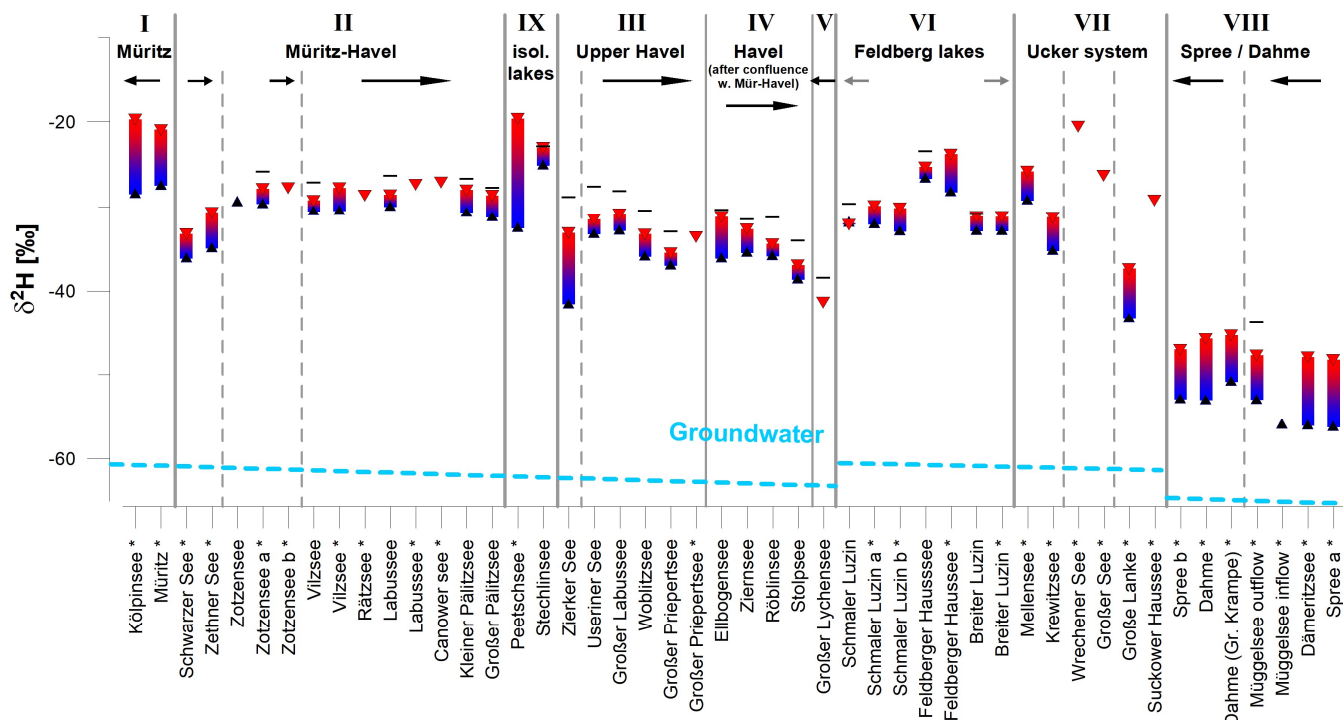


385

Figure 5: Time-series of  $\delta^2\text{H}$  and  $\delta^{18}\text{O}$  values of water samples taken from 1 m depth at deepest water depths in lakes connected to the Müritz-Havel and Upper Havel river system and the Feldberg lakes between March and October 2020. [Complementary water temperatures for each data point are available at PANGAEA.](#)



390 Figure 6: (a)  $\delta^{2}\text{H}$  and (b)  $\delta^{18}\text{O}$  values from samples taken at Zierker See (ZIS), Großer Priepertsee (PRI), Ellbogensee (ELL), and Röblinsee (ROB). For locations of samples refer to Table 3 and Fig 2. White squares and black squares for ELL mark samples before and after the confluence with the Upper Havel, respectively.



395 **Figure 7: Seasonal variability of  $\delta^2\text{H}$  values between spring (blue triangles) and summer (red triangles), framing the growing season**  
**of most aquatic and terrestrial plants. Additional data for autumn (black lines) where abundant, indicating the full seasonal isotope**  
**amplitude. in s** **Samples taken at lake shores (\*) and at buoys (1 m depth). Data** **Seasonal data represent samples taken in for spring**  
**and summer were taken in March, and June-/July, and October, respectively. Arrows mark surface (black) and subsurface flow**  
**(grey) direction. Triangles mark single data points. Roman numerals indicate geographical clusters as described in section 2. Vertical**  
**grey dashed line indicates sub-branches of these clusters (see Fig. 2). Light blue dashed line indicates approximate NW-SE trend in**  
**groundwater  $\delta^2\text{H}$  values according to Richter, 1987 and Richter and Kowski (1990).**

400

405

410

**Table 1: Parameters of lakes with shore sampling spots. Samples taken from 40-60 cm below water surface. Yellow dots in Fig. 1. Trophy class according to LAWA (2014) with year of most recent evaluation. Data from the respective German states were provided by local authorities (Landesamt für Umwelt Brandenburg, the Ministry of Agriculture and Environment Mecklenburg-Vorpommern, and Berliner Senatsverwaltung).**

Name	ID	Lat. [°N]	Long. [°E]	Sampl date I	Sampl date II	Area [ha]	Max depth [m]	Vol. [Mio m <sup>3</sup> ]	Res. time [a]	Catchment [km <sup>2</sup> ]	Trophy index / class / year
Kölpinsee	KOL	53.480486	12.602401	10 Mar	19 Jul	2009	30.0	71.8	0.930	906	2.2 / m2 / 2019
Müritz (Outer Müritz)	MUR	53.454812	12.609953	10 Mar	19 Jul	10201	29.2	674.9	10.1	735	1.8 / m1 / 2020
Schwarzer See	SCH	53.228292	12.788853	10 Mar	19 Jul	182	34.2	22.0	23.2	15	2.4 / m2 / 2020
Zethnersee	ZET	53.207225	12.789568	10 Mar	19 Jul	38.5	6.2	1.5	nd	20	3.1 / e2 / 2017
Peetschsee	PEE	53.205068	12.807274	10 Mar	19 Jul	18.2	10.6	0.8	nd	1	3.1 / e2 / 2016
Zotensee a	ZOT	53.234774	12.811522	-	19 Jul	149.5	21.4	10.1	0.152	116	3.3 / e2 / 2017
Zotensee b	ZOT	53.237293	12.825709	10 Mar	19 Jul						
Vilzsee	VIL	53.206542	12.839634	10 Mar	19 Jul	200.2	21.7	15.9	0.229	147	3.2 / e2 / 2017
Rätzsee	RAT	53.223299	12.867060	-	19 Jul	307.4	11.5	17.9	4.064	33	2.6 / e1 / 2020
Labussee	LAB	53.200965	12.873554	-	19 Jul	258.3	26.4	18.3	0.223	210	2.9 / e1 / 2014
Canower See	CAN	53.198937	12.916247	-	19 Jul	50.3	6.5	1.8	0.023	216	2.8 / e1 / 2020
Großer Priepertsee	PRI	53.219635	13.039599	-	19 Jul	105.2	26.7	11.4	0.163	412	3.2 / e2 / 2015
Schmaler Luzin a	SLU	53.325860	13.441056	08 Mar	16 Jul	146.2	33.5	21.2	3.359	30	1.4 / o / 2018
Schmaler Luzin b	SLU	53.341266	13.456269	08 Mar	16 Jul						
Feldberger Haussee	FEH	53.336906	13.441924	08 Mar	16 Jul	132.0	12.5	7.7	3.050	6	2.1 / m2 / 2018
Breiter Luzin	BLU	53.361765	13.502401	08 Mar	16 Jul	337.3	58.3	76.9	16.25	23	1.9 / m1 / 2018
Mellensee	MEL	53.290549	13.531495	08 Mar	16 Jul	73	18.3	5.4	5	93	2.1 / m2 / 2019
Krewitzsee	KRE	53.289324	13.531882	08 Mar	16 Jul	57	18.8	4.1	1	117	2.3 / m2 / 2019
Wrechener See	WRE	53.368161	13.531557	-	16 Jul	44.9	4.0	0.9	nd	12	2.6 / e1 / 2019
Großer See	GRO	53.391470	13.580108	-	16 Jul	357	20	24	nd	69	3.2 / e2 / 2017
Suckower Haussee	SUC	53.155456	13.847490	-	16 Jul	27	6.0	nd	nd	nd	2.7 / e1 / 2018
Oberrucker See (Gr. Lanke)	ORU	53.149541	13.854400	08 Mar	16 Jul	540	28.5	57	4	329	1.8 / m1 / 2017
River Spree b	SPREE	52.450164	13.567648	19 Mar	13 Jul						
River Dahme	DAHME	52.421870	13.585099	19 Mar	13 Jul						
Große Krampe	GRK	52.407561	13.666272	19 Mar	13 Jul	68	5.6	nd	nd	nd	nd
Müggelsee c (outflow)	MUG	52.444420	13.626031	19 Mar	13 Jul	746	7.7	36.6	0.14	<del>67907000</del>	--/ e12 / 2011
Müggelsee b	MUG	52.446808	13.638464	19 Mar	13 Jul						
Müggelsee a	MUG	52.448213	13.653171	19 Mar	13 Jul						
Müggelsee (inflow)	KLM	52.432557	13.676486	19 Mar	-						

Dämeritzsee	DAM	52.425817	13.730797	19 Mar	13 Jul	102.7	5.7	2.7	0.01	nd	--/ <del>e2p1</del> / 2011
<u>River</u> Spree a	SPREE	52.398384	13.747033	19 Mar	13 Jul						

420

425

430

435

**Table 2: Parameters of lakes equipped with buoys. Samples taken from 1 m below water surface. Orange dots in Fig. 1. Trophy class according to LAWA (2014) with year of most recent evaluation. Data from the respective German states were provided by local authorities (Landesamt für Umwelt Brandenburg, the Ministry of Agriculture and Environment Mecklenburg-Vorpommern, and Berliner Senatsverwaltung).**

Name	ID	Lat. [°N]	Long. [°E]	Trophy index /class / year	Lake area [ha]	Vol. [Mio m <sup>3</sup> ]	Catch ment [km <sup>2</sup> ]	Res. time [a]	Sampl. / max depth [m]	Sampling dates 2020
Zotzensee	ZOT	53.244500	12.810111	3.3 / e2 / 2017	149.5	10.1	116	0.152	20 / 21	18 Mar, 26 May, 30 Jun, 03 Aug, 01 Sep, 06 Oct
Vilzsee	VIL	53.209231	12.842569	3.2 / e2 / 2017	200.2	15.9	147	0.229	14 / 21	18 Mar, 26 May, 30 Jun, 03 Aug, 01 Sep, 06 Oct
Labussee	LAB	53.206569	12.899061	2.9 / e1 / 2014	258.3	18.3	210	0.223	17 / 26	17 Mar, 26 May, 30 Jun, 03 Aug, 01 Sep, 05 Oct
Kl Pälitzsee (E basin)	KPA	53.202269	12.960511	2.9 / e1 / 2014	132.9	7.0	224	0.075	22 / 26	19 Mar, 27 May, 02 Jul, 06 Aug, 03 Sep, 05 Oct
Gr Pälitzsee (N basin)	GPA	53.202261	12.990519	2.6 / e1 / 2014	82.4	6.5	242	0.077	13 / 15	19 Mar, 27 May, 02 Jul, 06 Aug, 03 Sep, 05 Oct
Stechlinsee	STE	53.147460	13.031148	2.2 / m2 / 2019	412	99.6	26	65.0	69 / 70	17 Mar, 25 May, 01 Jul, 04 Aug, 10 Sep, 06 Oct

Zierker See	ZIS	53.365950	13.045639	3.7 / p1 / 2018	351.0	5.7	23	1.128	2 / 3	17 Mar, 27 May, 29 Jun, 05 Aug, 03 Sep, 06 Oct
Useriner See	USE	53.332739	12.967211	2.8 / e1 / 2018	376.4	17.4	161	0.725	8 / 10	17 Mar, 28 May, 29 Jun, 05 Aug, 01 Sep, 06 Oct
Großer Labussee	GLA	53.312300	12.954881	2.8 / e1 / 2018	335.6	13.8	176	0.559	8 / 12	17 Mar, 27 May, 29 Jun, 03 Aug, 03 Sep, 05 Oct
Woblitzsee	WOB	53.284919	12.982481	3.3 / e2 / 2015	504.5	19.8	346	0.345	4 / 7	17 Mar, 27 May, 29 Jun, 03 Aug, 03 Sep, 04 Oct
Großer Priepertsee	PRI	53.221431	13.036339	3.2 / e2 / 2015	105.2	11.4	412	0.163	16 / 27	18 Mar, 26 May, 01 Jul, 06 Aug, 03 Sep, 08 Oct
Ellbogensee	ELL	53.207319	13.038950	2.9 / e2 / 2015	174.0	13.4	618	0.103	14 / 18	18 Mar, 26 May, 02 Jul, 06 Aug, 03 Sep, 08 Oct
Ziernsee	ZIE	53.205981	13.074319	2.8 / e1 / 2013	112.0	6.8	634	0.052	12 / 13	18 Mar, 26 May, 02 Jul, 06 Aug, 03 Sep, 08 Oct
Röblinsee	ROB	53.185311	13.120869	3.0 / e2 / 2017	87	3.3	729	7.0	7 / 8	19 Mar, 25 May, 01 Jul, 04 Aug, 31 Aug, 05 Oct
Stolpsee	STO	53.171819	13.221836	3.0 / e2 / 2017	371	24.7	1126	3.0	11 / 13	19 Mar, 25 May, 29 Jun, 04 Aug, 31 Aug, 07 Oct
Großer Lychensee	GLY	53.202550	13.283633	3.3 / e2 / 2017	282	17.6	175	3.0	19 / 19	--- , 25 May, 29 Jun, 04 Aug, 31 Aug, 07 Oct
Schmaler Luzin	SLU	53.318739	13.435600	1.4 / o / 2018	146.2	21.2	30	3.359	32 / 34	19 Mar, 28 May, 30 Jun, 05 Aug, 01 Sep, 08 Oct
Feldberger Haussee	FEH	53.347531	13.440081	2.1 / m2 / 2018	132.0	7.7	6	3.050	12 / 13	19 Mar, 28 May, 30 Jun, 05 Aug, 01 Sep, 08 Oct
Breiter Luzin	BLU	53.358181	13.465839	1.9 / m1 / 2018	337.3	76.9	23	16.254	56 / 58	19 Mar, 28 May, 30 Jun, 05 Aug, 01 Sep, 08 Oct

440

445 **Table 3: Sampling locations for spatial campaigns in Zierker See (ZIS), Großer Priepertsee (PRI), Ellbogensee (ELL) and Röblinsee (ROB). Samples #1 are identical with buoys as in Table 2 and taken from 1 m below water surface. White dots in Fig. 2.**

Sampling date	Location	Latitude [°N]	Longitude [°E]	Secchi Depth [m]	Water depth at sampl. site [m]
29.09.2020	ZIS 1	53.365975°	13.045650°	0.45	2.7
29.09.2020	ZIS 2	53.371400°	13.040172°	0.35	1.3
29.09.2020	ZIS 3	53.362697°	13.025783°	0.4	1.3
29.09.2020	ZIS 4	53.349753°	13.030467°	0.45	0.7
29.09.2020	ZIS 5	53.357917°	13.042639°	0.4	0.8
29.09.2020	ZIS 6	53.360944°	13.035014°	0.5	1.95
29.09.2020	PRI 1	53.221492°	13.036342°	1	16
29.09.2020	PRI 2	53.225261°	13.044003°	1.1	> 10
29.09.2020	PRI 3	53.235164°	13.049375°	1	2.2
29.09.2020	PRI 4	53.229672°	13.040261°	1	5

29.09.2020	PRI 5	53.224444°	13.038806°	1.1	> 10
29.09.2020	PRI 6	53.224444°	13.038806°	1.1	7.2
29.09.2020	PRI 7	53.219894°	13.037950°	1.1	9.2
30.09.2020	ELL 1	53.207383°	13.038944°	1.8	14.3
30.09.2020	ELL 2	53.215461°	13.027700°	1.85	6.3
30.09.2020	ELL 3	53.209814°	13.018661°	1.9	10.5
30.09.2020	ELL 4	53.213000°	13.036328°	1.9	6.3
30.09.2020	ELL 5	53.209417°	13.033500°	1.75	8.2
30.09.2020	ELL 6	53.200639°	13.038172°	1.7	6
30.09.2020	ROB 1	53.185361°	13.120836°	1.2	5.3
30.09.2020	ROB 2	53.185428°	13.113164°	1.2	1.5
30.09.2020	ROB 3	53.182275°	13.109422°	1.2	2.8
30.09.2020	ROB 4	53.182753°	13.118769°	1.1	5.4
30.09.2020	ROB 5	53.183917°	13.115953°	1.2	5.8
30.09.2020	ROB 6	53.183853°	13.130997°	1.2	2.5